J. Chem. Sci. (2019) 131:120
https://doi.org/10.1007/s12039-019-1707-5

REVIEW ARTICLE

Special Issue on 150 years of the Periodic Table

Chemical bonding in Period 2 homonuclear diatomic molecules: a comprehensive relook

A DAS and E ARUNAN*

Department of Inorganic and Physical Chemistry, Indian Institute of Science, Bangalore 560012, Karnataka, India

E-mail: arunan@iisc.ac.in

MS received 14 October 2019; revised 28 October 2019; accepted 30 October 2019; published online 5 December 2019

Abstract. Theoretical and experimental studies of bonding in the main group homonuclear diatomic molecules have been pursued for many years, and they possess serious challenges for scientists. Most of the early experimental work have been carried out by Herzberg.[1,2] We take a relook at the bonding motifs of Period 2 homonuclear diatomic molecules (from Li_2 to Ne_2) using varieties of quantum chemical tools, commonly used for intermolecular bonding/interactions now. The methods employed include Atoms in Molecules (AIM), Non-covalent Index plot (NCI), Electrostatic potential (ESP), and Potential Acting on one Electron in a Molecule (PAEM). The spectroscopic constants i.e., equilibrium bond distances (r_e), harmonic frequencies (ω), bond dissociation energies (D_e) have all been evaluated using high-level *ab initio* methods and critically compared with the experimental results. Multi-reference calculations (CASSCF) on B_2 and C_2 have been carried out as they have a large number of low lying electronic states. Bonding within these homonuclear diatomic molecules show all the diversities that are encountered in inter/intra-molecular bonding in chemistry. Based on the AIM analysis, these 8 homonuclear diatomic molecules could be divided into three different groups, based on the correlation between binding energy and the electron density at the bond critical point. However, PAEM/ESP analysis allows us to analyse all eight of them as one group having a good correlation between binding energy and the PAEM/ESP at the critical point between the two atoms. Our results highlight the arbitrariness in relying on some computational tools to characterize a bond as covalent (shared) or ionic/electrostatic (closed). In contrast, they also show the usefulness of the various methods in exploring similarities and differences in bonding. We propose that from Li_2 to Ne_2, all homonuclear diatomic molecules are bound by 'chemical bonds'.

Keywords. Covalency; Iconicity; van der Waals interaction; Atoms in molecules; electrostatic potential.

1. Introduction

Bonding within a molecule is generally considered to be well understood and there has been a greater focus on intermolecular bonding involving all group elements in the last decade or so. Until recently, all intermolecular interactions (chemists were hesitant to say intermolecular bonding) were divided into hydrogen bonding and van der Waals interactions and one can already see the confusion in terminology. Hydrogen bonding could readily be recognized in H_2O and DNA, the molecules of life. However, it was not so simple to understand, leading to a continuous debate on the nature of hydrogen bonding. At the beginning of this decade, IUPAC came up with a modern definition of the hydrogen bond.[3,4] With the periodic table having 118 elements today, it is but natural to ask why only 'hydrogen bond'. This question has now led to the observation of halogen bonding,[5–8] chalcogen bonding,[9–12] pnictogen bonding,[13–15] carbon/tetrel bonding,[16–20] triel bonding[21] and also lithium[22,23] and beryllium bonding.[24,25] Though, all these names have been given, the forces leading to these bonds are all the same. Electrostatic interactions between permanent

*For correspondence

Electronic supplementary material: The online version of this article (https://doi.org/10.1007/s12039-019-1707-5) contains supplementary material, which is available to authorized users.

and induced multipoles, dispersion, exchange repulsion and charge-transfer/covalency all contribute to varying extents. It is generally assumed that all but the last terms are 'physical forces' and covalency is a 'chemical force'. For terminology, chemical force led to 'chemical bond' formation and physical forces seem to have led to 'interactions', perhaps just confusion.

It dawned on us recently that bonding in Period 2 homonuclear diatomic molecules could cover this whole range found in inter/intra-molecular bonding, providing us a motive for this relook. The precise bonding nature of Period 2 diatomic molecules (Li_2 to Ne_2) is quite intriguing. A large variety of spectroscopic phenomenon is observed for these diatomic molecules, and the accurate description of the bonding nature is of principal importance. Interestingly, despite being their small size, these molecules are "tough nut to crack" by theoreticians and experimentalists. In terms of high-level theoretical calculations, there are a large number of papers and reviews dealing exclusively or predominately with these molecules, in the literature.[26–35]

The lithium dimer (Li_2) is the second smallest stable homonuclear dimer next to H_2. Spectra of Li_2 were observed and analysed in the 1930s. The evidence of Bose-Einstein Condensate in $^7Li_2$ by Bradley and coworkers[36,37] in 1995 has drawn a substantial amount of interest in this system. It is considered a covalent molecule, though the bond is much weaker (82 kJ/mol) than the covalent bond in H_2 (436 kJ/mol).

The study of the next simplest dimer (Be_2), was carried out by Herzberg.[38] These attempts failed to produce Be_2 and resulted only in observations of beryllium oxide (BeO).[39] Bondybey and English[40] first reported the gas phase spectrum in 1984, and established the fact that ground state of Be_2 is not repulsive with Be–Be bond distance is 2.45 Å. In 2009 Merritt, Bondybey and Heaven[41] with the advent of pulsed laser ablation techniques recorded and analysed all the bound vibrational levels of Be_2. Interestingly, the Be···Be bond was neither like Li_2 'covalent' nor like Ne_2 'van der Waals interaction'. It is precisely for this reason that 'a hydrogen bond' was proposed i.e. it was neither as strong as the O–H covalent bond in H_2O nor as week as the 'van der Waals interaction'.

Boron dimer (B_2) was first experimentally observed in 1940 by Douglas and Herzberg.[42] In a discharge in helium with a trace amount of boron trichloride, they could establish that B_2 was a stable molecule. On the basis of molecular orbital theory Douglas and Herzberg tentatively assigned this to the $^3\Sigma_u^-$ - $^3\Sigma_g^-$ transition. The optical absorption and ESR spectrum of B_2 reported by Graham and Weltner in 1976 confirm $^3\sum_g^-$ ground state.[43] Recent theoretical calculations on B_2 using fairly large basis sets and electron correlation established that the ground state of B_2 was $^3\Sigma_g^-$.[44,45]

There is considerable interest in the nature of the bonding in diatomic carbon (C_2). It has been observed during the photodissociation of acetylene and can be formed by the direct reaction of the C(^{3}P) atom with CH.[46–49] The spectroscopy of low lying electronic state is well known.[50–53] The C_2 molecule has been variously described as having a double bond,[54] triple bond[55] or a quadruple bond.[56,57] The nature of bonding in C_2 is still debated.

The most strongly bound diatom, N_2 certainly belongs to the most extensively studied systems. There are numerous studies on its ground state, lowest triplet and quintet states. Spectroscopic data and early quantum chemical calculations have been comprehensively reviewed by Lofthus and Krupenie[58] and Huber.[59] On the other hand, owing to the larger number of valence electrons, the number of low lying bound excited states of O_2 is much smaller than N_2 or C_2.

The interest in excited states of O_2 is large because of its importance in terrestrial chemistry and biochemistry. The most comprehensive review of the spectroscopy of O_2 has been given by Krupenie[60] and Matsunaga and Watanabe.[61] Further experimental data can be found in a book of Huber.[59] Electronic structure and spectrum of F_2 molecule have been published in early 1920's.[62,63] Raman spectrum of F_2 was measured by Andrychuk.[64] Absorption spectra of homopolar diatomic rare gas Ne_2 has been studied by Tanaka and Yoshino in 585–760 Å region.[65] They have identified 12 discrete band systems. The ground state of Ne_2 is stable with potential depth of D_e = 30.2 cm^{-1}.

We have also included LiH and HF (Heteronuclear dimers) in this review because the nature of interaction of these diatomic hydrides are different, former being 'more ionic' and the latter being 'more covalent'. The bonding in second row hydrides covers the complete range of Pauling's definition of ionic-covalent character.[66] Thus the dipole moment of HLi is −5.882 D in the sense H^-Li^+, while for HF the polarity is reversed, i.e., in the sense H^+F^-, and the magnitude of the dipole moment is 1.8195 D.[67]

This manuscript focuses on the bonding nature of homonuclear diatomic molecules based on the popular quantum chemistry tools. Much of the chemical information in this paper is derived from the analysis of molecular electron density (ρ). Bader[68] and Popelier[69] employed the electron density to build a rigorous QM basis for the definition of an atom in a molecule (AIM). The AIM theory primarily looks at the electron

density at every point around the nuclei of a molecule. Based on the electron density, we have calculated several other properties like an electronic population of the atom, delocalization index, etc. The AIM theory is a powerful method to predict the nature of the bond based on the electron densities at the bond critical point. In particular, several methods have been developed to characterize, intermolecular interactions as 'closed-shell' and 'shared-shell', and these can be related to 'ionic bond' or 'non-covalent interactions' and 'covalent bond' in chemistry.[70,71] It would not be an exaggeration to point out that understanding 'hydrogen bond' has motivated some of these efforts. The non-covalent index plot is primarily designed to study weak bonding interactions.[72–74]

In this manuscript, we report results for the homonuclear diatomic molecules from Period 2 using all these methods. Moreover, we have calculated potential acting on one electron molecular orbitals (PAEM-MO)[75–78] and the electrostatic potential (ESP) for the diatomic molecules. Interestingly, these methods provide a universal way to look at the bonds holding the Period 2 atoms together when they form a diatomic molecule. Discussion on HLi and HF have been included for comparison.

2. Computational details

Homonuclear diatomic molecules of Period 2 and HLi/HF were optimized using DFT (B3LYP), MP2, CCSD, and CCSD (T) methods with different basis sets. The calculations were performed using Gaussian 09[79] program. Multireference calculations were performed using Molpro 2015.1 version.[80] Atoms in molecules (AIM)[68] theory has been used to carry out electron density topological studies using AIMALL program.[81] The Wiberg bond order of the diatomic molecules have been calculated with the help of NBO 6.0.[82] Natural Resonance Theory (NRT)[83] was used to calculate the fraction of ionicity and covalency in the homonuclear diatomics and also LiH and HF molecules. By using the Multiwfn[84] program the Non Covalent Index (NCI)[74] plots were obtained with two functions, function 1 (on the X-axis) is the multiplication of the sign of the second eigenvalue (λ_2) of electron density Hessian matrix with the electron density (ρ)sign (λ_2)*ρ)] and function 2 (on Y-axis) reduced density gradient. NCI plot provides a way to differentiate between covalent bonds and van der Waals interactions. Potential acting on one electron in a molecule (PAEM) is also able to capture the differences between covalent and van der Waals interaction based on molecular orbital viewpoint. PAEM calculations are carried out using Multiwfn 3.6 program.[84]

3. Results and Discussion

3.1 *Geometric parameters*

The results from our calculations are presented in Tables 1, 2, and 3. The equilibrium bond distances and Wiberg bond order are presented in Table 1 calculated at CCSD(T)(Full)/aug-cc-pVTZ level, along with the experimental bond distances. They are in very good agreement, except for Be_2, which has a deviation of more than 0.1 Å. It was noted that the results for Be_2 vary widely with the level and basis set. The results at many different levels of calculations are given in the supporting information (Table ST1, Supplementary Information).

The bond distances are compared with twice the atomic, covalent and van der Waals radii and these lead to some trivial and some non-trivial conclusions. In Ne_2, the bond distance is very close to the sum of van der Waals radii. The only other molecule for which the experimental bond distance is close to the sum of radii is F_2 and for this, the agreement is with the sum of atomic radii and not with the sum of covalent radii. From B_2 to O_2, all have multiple bonds and hence appropriate covalent radii should be compared. As mentioned earlier, Be_2 has a bond distance that is less than the sum of its van der Waals radii but more than that of the covalent radii.

The Wiberg bond order calculated for these diatomic molecules vary from 0 for Ne_2 to 3.661 for C_2. For comparison, HLi, which is a typical ionic bonded molecule has a bond order of 0.2851 and HF, thought to be a 'covalent' molecule has a bond order of 0.6868. Beyond, Ne_2, the lowest bond order is calculated for Be_2, 0.1615.

It is interesting to note that the highest level of calculations, CCSD(T)(Full), are able to get the interatomic distances very close to the experimental values, for all the diatomic molecules of Period 2, irrespective of the nature of bonding. Clearly, modern quantum theory can explain chemistry in all circumstances well, despite the continuous debate on the nature of 'chemical bond', including that present in the simplest of all molecules, H_2.[85] The devil, indeed, is in the detail. We submit that all the atoms considered in this work are chemical, and all these homonuclear diatomic molecules are held together by 'chemical bonds'.

Table 1. Electronic ground state, Wiberg bond order, equilibrium bond distances for Period 2 dimers (aug-cc-pVTZ) and the sum of atomic, covalent and van der Waals radii (values are in Å)*.

	Ground state	Wiberg bond order	CCSD(T) (full)	Expt.	Atomic	Covalent	van der Waals
Li_2	$^1\sum_g^+$	1.0005	2.667	2.673	3.04	2.66	3.64
Be_2	$^1\sum_g^+$	0.1615	2.343	2.453	2.25	2.04	3.06
B_2	$^3\sum_g^-$	2.2734	1.587	1.590	1.66	1.70/1.56	4.16
C_2	$^1\sum_g^+$	3.6610	1.245	1.243	1.54	1.50/1.34/1.20	3.70
N_2	$^1\sum_g^+$	3.0332	1.101	1.098	1.42	1.42/1.20/1.08	3.08
O_2	$^3\sum_g^-$	2.0248	1.209	1.208	1.30	1.26/1.14	2.80
F_2	$^1\sum_g^+$	1.0044	1.414	1.412	1.42	1.28	2.70
Ne_2	$^1\sum_g^+$	0.0000	2.976	3.091*	3.08	1.34	3.20
HLi	$^1\sum^+$	0.2851	1.592	1.595	2.30	1.65	3.02
HF	$^1\sum^+$	0.6868	0.919	0.918	1.49	0.96	2.55

*Ref[86].

Bond lengths are taken from NIST database except where a superscript appear.

All radii are taken from the book 'Elements' by Emsley.[87]

Table 2. Vibrational frequencies (cm^{-1}) (without anharmonic correction) for Period 2 dimers (aug-cc-pVTZ).

	DFT	MP2	CCSD	CCSD(T)	CCSD (T,full)	*Experiment
Li_2	343	341	345	345	343	351
Be_2	287	108	29	207	384	271
B_2	1006	1098	1028	1038	1083	1051
C_2	1875	1875	1877	1841	1878	1855
N_2	2448	2187	2419	2340	2370	2358
O_2	1626	1455	1658	1575	1593	1580
F_2	1050	1004	1011	917	925	892
Ne_2	30	29	30	33	38	30
HLi	1418	1414	1386	1387	1405	1405
HF	4073	4123	4170	4126	4141	4138

*Experimental vibrational frequencies are taken from NIST database.

Table 3. Dissociation energies (kJ/mol) for Period 2 dimers (aug-cc-pVTZ). Zero-point energies are given in the parenthesis.

	DFT	MP2	CCSD	CCSD(T)	CCSD (T,full)	Experiment
Li_2	87.4(2.1)	72.3(2.0)	99.6(2.1)	99.6(2.1)	103.4(2.1)	82.4[a]
Be_2	17.8(1.7)	4.4(0.6)	0.7(0.2)	4.2(1.2)	34.7(2.3)	$11.1 + 0.02$[b]
B_2	251.2(6.0)	266.0(6.6)	225.3(6.1)	225.3(6.2)	247.5(6.5)	290[c]
C_2	498.9(11.2)	634.5(11.2)	506.9(11.2)	506.8(11.0)	459.1(11.2)	618.3 ± 15.4[c]
N_2	957.8(14.6)	964.9(13.1)	873.9(14.5)	873.5(14.0)	897.8(14.2)	944.84 ± 0.10[c]
O_2	515.3(9.7)	531.3(8.7)	448.9(9.9)	448.4(9.4)	462.5(9.5)	498.36 ± 0.17[c]
F_2	155.2(6.3)	175.1(6.0)	123.3(6.0)	122.4(5.5)	128.7(5.5)	158.670 ± 0.096[c]
Ne_2	0.1(0.2)	0.3(0.2)	0.4(0.2)	0.4(0.2)	0.6(0.2)	0.35[d]
HLi	244.8(8.5)	216.6(8.5)	238.1(8.3)	238.1(8.3)	243.7(8.4)	238.039 ± 039[c]
HF	582.0(24.4)	601.1(24.7)	574.4(24.9)	574.4(24.7)	579.0(24.8)	569.680 ± 0.011[c]

[a] Ref[88], [b]Ref[41], [c]Ref[89], [d]Ref[86].

Table 4. Types and characteristic of critical points (cps) based on the rank and signature of the hessian matrix.

(Rank, Signature)	Types of critical points	Curvature
(3, −3)	Nuclear critical point (NCP)	All negative, local maxima
(3, −1)	Bond critical point (BCP)	Two negative, one positive
(3, +1)	Ring critical point (RCP)	One negative, two positive
(3, +3)	Cage critical point (CCP)	All positive, local minima

3.2 *Vibrational frequencies and dissociation energies*

Theoretical frequencies calculated at various level are compared with experimental values in Table 2. The results are similar to those discussed above and except for a specific problem at CCSD level for Be_2, other numbers do look reasonable. A detailed analysis of method and basis set dependencies of Be_2 geometry has been provided in Table ST1 (Supplementary Information). Considering the fact that these are harmonic frequencies, most numbers look reasonable. In particular, the values for Li_2 and Ne_2, in comparison with Be_2 highlight an important point. Li_2 considered covalent and Ne_2 bound by London dispersive forces are both handled well by all methods. However, for Be_2, the results show a large variation depending on the methods. Both in terms of distance and vibrational frequency, DFT appears to be doing better than MP2 and CCSD methods for Be_2. A detailed discussion on these diatomics is given in the later sections.

The dissociation energies reported for the homonuclear diatomic molecule reinforces the points mentioned above. If one looks for quantitative comparison, the differences between experimental and computed values are somewhat larger compared to data presented in Tables 1 and 2. However, the fact that the dissociation energies, given in Table 3, range from 0 to 1000 kJ mol^{-1} and these are computed reasonably well, shows that the quote "The fundamental laws necessary for the mathematical treatment of a large part of physics and the whole of **chemistry** are thus completely known, and the difficulty lies only in the fact that application of these laws leads to equations that are too complex to be solved" by Dirac was indeed prophetic. For N_2, O_2, F_2, DFT reproduces the dissociation energies much better than the other methods, especially the CCSD methods. A comparison of the percentage errors are given in the Supplementary Information (see SF1). For HLi and HF calculated dissociation energies from all the methods are in excellent agreement with the experimental values.

3.3 *Atoms in molecules analysis*

Topological study of electron density (ρ)[68] helps us look deeper into the nature of chemical bonds. Any point in space where all the first-order partial derivative of electron density vanishes is termed as a critical point (cp). The topological feature of such points are characterised in terms of the rank and signature of the Hessian matrix. The rank is defined as the number of non-zero eigenvalues of the Hessian matrix and signature as the algebraic sum of the sign of the non-zero eigenvalues. Based on this a scalar function can have four types of critical points, as shown in Table 4.

Most of the stable nuclear configurations critical points are of rank three. In a few exceptions, degenerate cps with rank < 3 are observed. A degenerate critical point is unstable and a small change in electron density caused by slight displacement in nuclear configuration makes it vanish or changes it to stable cps of rank three. We have observed the degenerate critical points with rank 2 in C_2 for CCSD(T) wave functions. The AIM parameters calculated for the diatomic molecules have been summarized in Table 5. The method and basis set dependence of these parameters are summarized in Tables ST2–ST9 (Supplementary Information). Major conclusions from this analysis do not depend on the method and basis set. Some details do vary and they are discussed in this section.

To understand how the electron density varies between the two atoms, having a chemical bond, we have plotted electron density (ρ) and gradient norm of electron density ($|\nabla\rho|$) variation along the internuclear axis of N_2 (Figure 1). Electron density at the midpoint of N–N bond is minimum, so its first derivative goes to zero at that point resulting in a bond critical point.

3.4 *Electron density vs. binding energy correlation*

Bader[68] showed that the electron density at BCP is a good indicator of strength of the bonds. In this review,

Table 5. Properties calculated from atoms in molecules analysis. Wave functions used for the calculations are evaluated at CCSD (T)(full)/aug-cc-pVTZ level. (In case of C_2 wave function at CCSD/aug-cc-pVTZ level used for calculation).

Diatomic molecules	ρ(r)	$\nabla^2\rho$	$\lambda_1 = \lambda_2$	λ_3	$\lvert\lambda_1\rvert/\lambda_3$	V	G	|V|/G
*Li_2	0.0139	+0.0089	−0.0054	+0.0197	0.274	−0.0063	+0.0043	1.47
Be_2	0.0373	−0.0462	−0.0275	+0.0088	3.125	−0.0151	+0.0018	8.39
*B_2	0.1247	+0.0839	−0.0805	+0.2449	0.329	−0.2582	+0.1396	1.85
*C_2	0.3160	−0.0161	−0.2197	+0.4232	0.519	−1.0496	+0.5228	2.01
N_2	0.7204	−3.5009	−1.9419	+0.3829	5.072	−2.1117	+0.6182	3.42
O_2	0.5505	−0.9375	−1.5281	+2.1187	0.721	−1.1771	+0.4713	2.50
F_2	0.3004	+0.2013	−0.7351	+1.6716	0.440	−0.4720	+0.2612	1.81
Ne_2	0.0023	+0.0144	−0.0025	+0.0194	0.129	−0.0022	+0.0029	0.76
HLi	0.0402	+0.1704	−0.0607	+0.2919	0.208	−0.0431	0.0429	1.00
HF	0.3735	−3.5009	−2.6993	+1.8977	1.422	−1.0381	0.0814	12.75

*Presence of Non-nuclear attractor (NNA), with two bond critical points (BCP), ρ(r) is the electron density, $\nabla^2\rho$ is Laplacian of electron density, λ_1 and λ_3 are the first and third eigenvalue of Hessian matrix, all at intermolecular BCP, V potential energy density, G kinetic energy density. All the quantities are in atomic units.

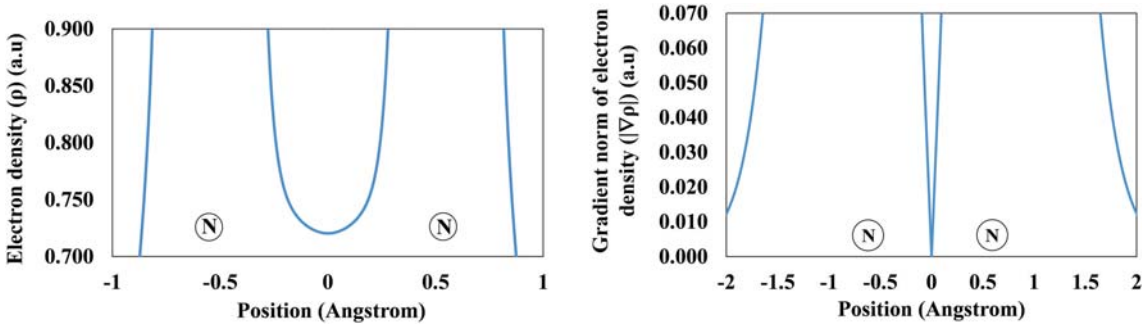

Figure 1. Electron density (ρ), gradient norm of electron density (|∇ρ|) plot for N_2. (Y-axis: Values are in a.u, X-axis: Values are in angstrom).

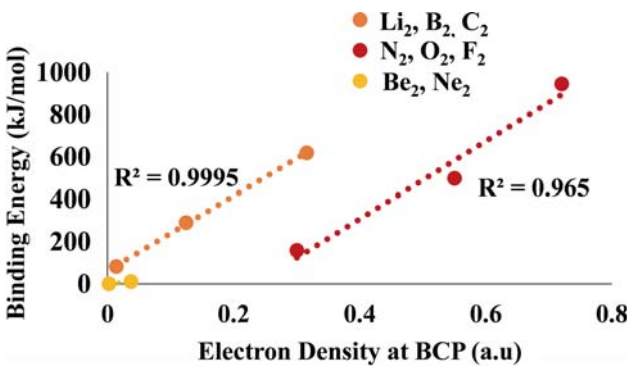

Figure 2. Binding energy (kJ/mol) vs. electron density plot (a.u) for Period 2 dimers.

we have taken 8 homonuclear diatomic molecules, bonding nature of these diatomic molecules will be discussed in details in the next section. We have divided these diatomic molecules into three different classes. Li_2, B_2, and C_2 show non-nuclear attractors (NNA) along the internuclear axis. Ne_2 and Be_2 are quite similar, both have dispersion dominated interactions. On the other hand, N_2, O_2 and F_2 are typical examples of covalent bonds. In can be seen from Figure 2 that such a division is logical and within these three classes of molecules, binding energy correlates well with the electron density. Without such grouping, the correlation between electron density and binding energy is poor leading to a decreased R^2 value of 0.8, as shown in Figure SF2 (Supplementary Information).

3.5 *Differentiation between closed and shared shell interaction based on atoms in molecules topological analysis*

Sign of Laplacian at the bond critical point has been used to differentiate between closed and shared shell interaction. Closed shell interactions are characterized by positive Laplacian ($\nabla^2\rho > 0$) whereas negative Laplacian ($\nabla^2\rho < 0$) indicates shared shell interaction. Soon, it was realized that this criterion could be misleading and Sosa *et al.*,[70] introduced another criterion based on the ratio of $|\lambda_1|/\lambda_3$ i.e., the first and

Table 6. Defined parameters to differentiate between kinds of interaction from Atoms in Molecules theory.

Criterions	$\nabla^2\rho$	$\lvert\lambda_1\rvert/\lambda_3$	$\lvert V\rvert/G$
Closed (Ionic, van der Waals)	Positive	0–0.25	0–1.00
Shared (Covalent)	Negative	1 and above	2.00 and above
Intermediate	–	0.25–1.00	1.00–2.00

third eigenvalue of the Hessian matrix. For diatomic molecules, $\boldsymbol{\lambda_1}$ and $\boldsymbol{\lambda_2}$ are degenerate. $\boldsymbol{|\lambda_1|/\lambda_3}$ less than 0.25 indicated a closed shell and greater than 1 indicated a shared shell interaction. Values in between 0.25 and 1 are regarded as interaction of intermediate kind. Cremer and Karka[71] proposed another criterion based on potential (V) and kinetic (G) energy density ratio. For closed-shell interaction, $\boldsymbol{|V|/G} < 1$ and for shared shell $\boldsymbol{|V|/G} > 2$. $\boldsymbol{|V|/G}$ in between the limits proposed as intermediate kind of interaction. For the sake of simplicity, we have tabulated all these criteria in Table 6 and their applications to the diatomic molecules in Table 7.

The data presented in Table 7 highlight the arbitrariness of these criteria for the 8 homonuclear diatomic molecules from Period 2. For HLi and HF, all three criteria lead to the expected outcome, though for HLi, |V|/G is at the border between closed and intermediate. Only for three of the eight cases, Be_2, N_2 and Ne_2, all three criteria lead to the same conclusion. However, Be_2 is shown to have 'shared-shell interaction' and Ne_2, as expected, a closed-shell interaction. In the previous section, it was pointed out that Be_2 and Ne_2 are similar and hence both would have 'closed-shell interaction. While it was expected that all the other 7 homonuclear diatomics would have 'shared-shell' interaction, only N_2 fulfilled all three criteria. Both Li_2 and F_2 appear similar, having a 'closed-shell interaction' based on $\nabla^2\rho$, and intermediate interaction based on the other two criteria. The $\nabla^2\rho$ for F_2 has a large positive value, indicating electron depletion in bond critical point, the other two criterion falls in the intermediate kind. $\nabla^2\rho$ has a large negative value for O_2 but $\boldsymbol{|\lambda_1|/\lambda_3}$ ratio falls in the intermediate range. |V|/G ratio is more than 2 irrespective of the nature of wave function. Li_2, B_2 and C_2 show NNA along the internuclear axis, so the parameters derived at the BCP may not represent the interaction between the atoms. However, the electron density is nearly flat and the densities at both BCPs and the NNA in between them are very close in value. Ne_2 expectedly shows closed-shell interaction in all three parameters. A bar diagram showing |λ1|/λ3 and |V|/G for all diatomic molecules is given in Figure SF3 (Supplementary Information).

Table 7. Nature of interaction in Period 2 homonuclear dimers using criterions defined in Table 6.

Criterions	$\nabla^2\rho$	$\lvert\lambda_1\rvert/\lambda_3$	$\lvert V\rvert/G$
Li_2	Closed	Intermediate	Intermediate
Be_2	**Shared**	**Shared***	**Shared**
B_2	Closed	Intermediate	Intermediate
C_2	Shared	Intermediate	Shared
N_2	**Shared**	**Shared**	**Shared**
O_2	Shared	Intermediate	Shared
F_2	Closed	Intermediate	Intermediate
Ne_2	**Closed**	**Closed**	**Closed**
HLi	Closed	Closed	Closed[#]
HF	Shared	Shared	Shared

*In MP2/aug-cc-pVTZ method value is 0.709; [#]The value is 1.004 and it is right at the border of shared and intermediate.

3.6 *Properties of the atoms*

The Atoms in Molecules approach naturally allows one to estimate the number of electrons within the boundary of atoms in a molecule and compare it with the number of electrons in the independent atom. Such an analysis is presented in Tables 8 and 9 for the homonuclear diatomics without and with non-nuclear attractors in between. This gives a very different picture of all these molecules. N_2 with three covalent bonds has the largest percentage of electrons staying within its boundary and that is a very high 78%. Not surprisingly, Ne_2 retains almost all the electrons with itself and one has to use more decimals to get an accurate picture, 99.95%. Another surprising result of this analysis is that Be_2 has more delocalization (10%) than F_2 (7%). Clearly this difference is due to the difference in electronegativity. All the homonuclear diatomic molecules from Period 2, having no NNA, have a small percentage of delocalization.

A similar analysis for the Li_2, Be_2 and C_2 give results in stark contrast with the other homonuclear

Table 8. Localization and delocalization data of diatomic molecules without NNA.

Diatomic molecules	N(A)	LI(A)	%Loc(A)	DI(A,A′)/2	%Deloc(A,A′)
Be_2	4.0	3.58	90	0.42	10
N_2	7.0	5.48	78	1.52	22
O_2	8.0	6.89	86	1.11	14
F_2	9.0	8.38	93	0.62	7
Ne_2	10.0	9.994	99.95	0.005	0.05

N(A): Average Number of Electrons in Atom A, LI(A): Average Number of Electrons Localized in Atom A, %Loc(A): Percentage of Average Number of Electrons in Atom A that are Localized in Atom A, DI(A,A′)/2: Average Number of Electrons in Atom A that are Delocalized (Shared) Between Atom A and Other Atoms of Molecule, % Deloc(A,A′): Percentage of Average Number of Electrons in Atom A That are Shared With Other Atoms of Molecule.

Table 9. Localization and delocalization data of diatomic molecules with NNA. (In case of C_2 wave function at CCSD/aug-cc-pVTZ level used for calculation).

Atoms	N(A)	LI(A)	%Loc(A)	DI(A,A′)/2	%Deloc(A,A′)
Li_2	2.37	2.07	87	0.30	13
NNA(Li_2)	1.26	0.79	63	0.47	37
B_2	4.55	3.51	77	1.04	23
NNA(B_2)	0.91	0.22	24	0.69	76
*C_2	5.61	4.51	80	1.10	20
*NNA(C_2)	0.78	0.16	20	0.62	80

diatomic molecules from Period 2. For these molecules, the NNA is treated as a nucleus as well and one could calculate the percentage of electrons localized and delocalized on nuclei and NNA, as shown in Table 9. Popelier has pointed out that electron density in these non-nuclear attractors are mostly delocalized. In case of the Li_2, 37% of electron density is delocalized in the NNA. Electron delocalization percentages in NNA of B_2 and C_2 are 76% and 80% respectively.

Electrons on boron atoms are the most delocalized (23%) Table 9. Properties of these NNA's are provided in Table ST10 (Supplementary Information). One could also compare the localized electrons in the two atoms with the total number of electrons, after molecule formation. This leads to the percentage delocalization of 31% for Li_2, 29.8% for B_2 and 24.8% for C_2, all higher than the other molecules. Though the bonding in these molecules has been interpreted as two bonds between the atom and NNA, we propose that the presence of NNA itself could be treated as the historic covalent bond, showing accumulation of electrons between the two atoms.

In order to ensure that the presence of NNA is not method/basis set dependent, we have evaluated the wave functions from several different levels of theory and basis sets. The presence of NNA in Li_2 can be seen irrespective of the methods and basis sets (Table 10), whereas for B_2 and C_2 presence and number of NNA's are method and basis set dependent (Tables 11 and 12). The highest single reference calculation at CCSD(T) level, confirms the presence of NNA for both C_2 and B_2. However, both B_2 and C_2, have fairly large number of low lying electronic states (Table ST12, Supplementary Information). Hence, to resolve this ambiguity we invoked the multi-reference CASSCF calculations. These results are presented in Table 13. At the highest level of multi-reference calculations carried out in this work, CASSCF with aug-cc-pvQZ basis set, there is no NNA for both these molecules! Along with the diatomic molecules, in a few rare cases NNA (3, −3) critical points are observed such as lithium, sodium and beryllium clusters.[90,91] Experimentally NNAs are recognized in solid silicon[92] and beryllium.[93] In 2011, Platts *et al.,* reported the presence NNA in the case of dimeric magnesium compound in Mg-Mg region.[94]

Table 10. Dependence on methods and basis sets for the number of non-nuclear attractors (NNA) in Li_2.

	HF	DFT(B3LYP)	MP2	CCSD	CCSD(T)
6-311G++(d,p)	1	1	1	1	1
cc-pVDZ	1	1	1	1	1
cc-pVTZ	1	1	1	1	1
cc-pVQZ	1	1	1	1	1
aug-cc-pVDZ	1	1	1	1	1
aug-cc-pVTZ	1	1	1	1	1
aug-cc-pvQZ	1	1	1	1	1

Table 11. Dependence on methods and basis sets for the number of non-nuclear attractors (NNA) in B_2.

	HF	DFT(B3LYP)	MP2	CCSD	CCSD(T)
6-311G++(d,p)	0	0	2	0	2
cc-pVDZ	2	2	2	0	2
cc-pVTZ	2	1	1	1	1
cc-pVQZ	2	2	2	2	1
aug-cc-pVDZ	2	2	2	0	2
aug-cc-pVTZ	2	2	1	1	1
aug-cc-pvQZ	2	2	2	2	1

Table 12. Dependence on methods and basis sets for the number of non-nuclear attractors (NNA) in C_2.

	HF	DFT(B3LYP)	MP2	CCSD	CCSD(T)
6-311G++(d,p)	1	0	0	0	2
cc-pVDZ	1	2	0	0	1
cc-pVTZ	1	1	1	1	1
cc-pVQZ	1	2	2	2	1
aug-cc-pVDZ	1	2	0	0	2
aug-cc-pVTZ	1	1	1	1	1
aug-cc-pvQZ	1	2	2	2	1

3.7 *Comparison between Li_2 and Be_2*

Bonding nature of first two simplest diatomic molecules is significantly different from each other. We have compared the bonding in Li_2 and Be_2 based on the parameters derived in the previous section. Non-covalent index (NCI) plots have been used in the same context. Results are summarized in Table 14.

Li_2 is 7 times more strongly bound than Be_2. On the contrary, electron density at bond critical point for Be_2 (0.0373 a.u) is greater than Li_2. A recent theoretical report[95] showed that Be–Be bond in radical ligand (L: Be–Be: L) becomes up to 300 times stronger than isolated Be_2. With L = [CN], the strength of the Be–Be bond was calculated to be 330 kJ/mol, strongest Be–Be bond reported in the literature so far.

The variation of electron density and gradient norm of electron density, along the bond axis have been plotted for Li_2 and Be_2 (Figure 3) using the Multiwfn 3.6 program. In the case of Li_2, the presence of electron density maximum in between Li–Li region is indicative of Non-nuclear attractor (NNA). We have not found any such NNA in Be_2 at the equilibrium bond distance. However, a slight change in bond distance could lead to NNA in between Be–Be bond. Laplacian of electron density at the bond critical point

Table 13. Number of NNA generated from CASSCF calculation on B_2 and C_2.

	B_2	C_2
6-311G++(d,p)	0	0
cc-pVDZ	0	0
cc-pVTZ	2	1
cc-pVQZ	0	0
aug-cc-pVDZ	0	0
aug-cc-pVTZ	2	1
aug-cc-pVQZ	0	0

for Li_2 is positive. Positive Laplacian indicates the 'closed-shell' interaction. The central subspace has a wide region characterized by a negative Laplacian thereby indicating a concentration of charge and a dominance of the stabilizing potential energy contribution in the Li–Li internuclear region. As a consequence, the properties at (3, −1) critical point are no longer directly related to the nature of Li–Li interaction.

On the other hand, in Be_2 a large negative portion (dotted red lines) in between the Be–Be nucleus which indicates electron accumulation in that region as can be seen from the variation of gradient norm of electron density ($|\nabla\rho|$) along the internuclear axis (Figure 4) and the 2D contour plot (Figure 5). Similar plots for HF and LiH are given in Supplementary Information (Figure SF5).

3.8 *Non-covalent index plot for Li_2 and Be_2*

The non-covalent interaction (NCI) method, which is also known as reduced density gradient (RDG) method, is a very popular method for studying weak interaction which actually deals with electron density ρ(r) and reduced density gradient s(r).

$$s(r) = \frac{1}{2(3\pi^2)^{1/3}} \frac{|\nabla\rho(r)|}{\rho(r)^{4/3}}$$

At the bond critical point where the first derivative of electron density goes to zero [$\nabla\rho(r) = 0$], the reduced density gradient also becomes zero. So the intra/intermolecular interaction can be identified using the plot of reduced density gradient and electron density. The sign of the second eigenvalue of the Hessian matrix (λ_2) is utilized to distinguish between types of interactions. $\lambda_2 < 0$ characterizes bonding interaction; $\lambda_2 > 0$ non-bonding interaction i.e. steric repulsion. Finally, van der Waals interactions are characterized by a negligible density overlap that gives $\lambda_2 \lesssim 0$. This method, called NCI plot, was developed by Yang's group.[72–74]

The NCI plot for Li_2 shows two troughs, almost overlapping (Figure 6). As previously discussed Li_2 has two bond critical points. Both the bond critical points have similar electron density, the two troughs are the result of two existing BCP's. In Be_2 NCI plot one trough is observed around −0.028 a.u.

Table 14. Comparison in bond length, bond dissociation energy, electron density at BCP (ρ) and Laplacian of electron density at BCP ($\nabla^2\rho$) of Li_2 and Be_2 (CCSD (T)(Full)/aug-cc-pVTZ).

	Bond length (Å)	Bond dissociation energy (kJ/mol)	ρ (a.u)	$\nabla^2\rho$ (a.u)
Li_2	2.673	82.4	0.0139	+0.0089
Be_2	2.453	11.1	0.0373	−0.0462

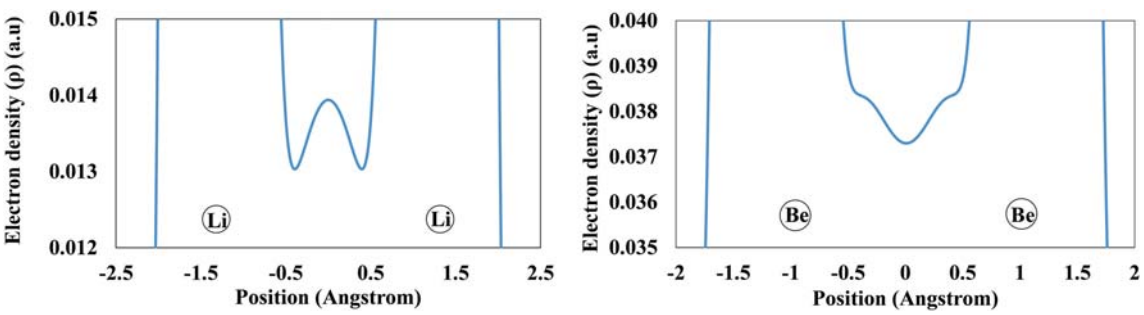

Figure 3. Variation of electron density (ρ) along the internuclear axis of Li_2 (left, with NNA) and Be_2 (right, without NNA).

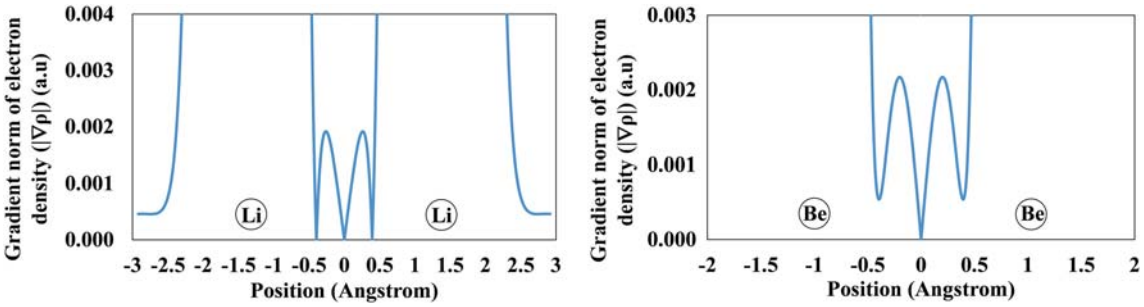

Figure 4. Variation of gradient norm of electron density ($|\nabla\rho|$) along the internuclear axis of Li_2 (left, with 3 critical points) and Be_2 (right, with one critical point).

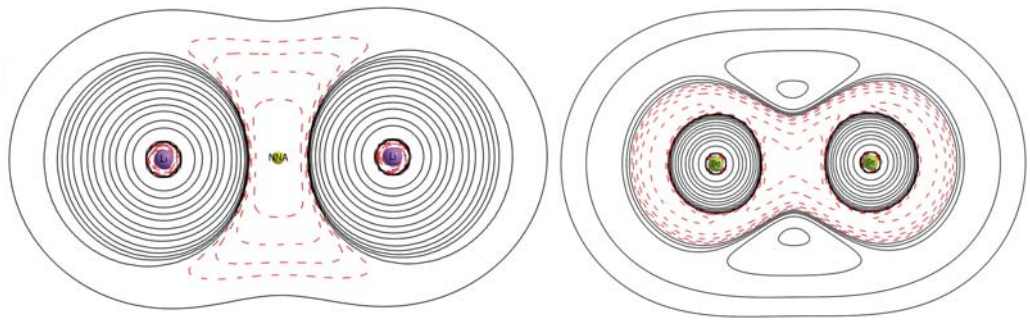

Figure 5. 2D contour plot of Laplacian of electron density of Li_2 (left) and Be_2 (right). Black solid lines denote positive values and red dotted lines denote negative values. Calculated using CCSD (T)/aug-cc-pVTZ level of theory.

3.9 *Comparison between N_2 and Ne_2 based on electron density contour map*

N_2 and Ne_2 belong to two different regimes of chemical bonding. Electron density at bond critical point of N_2 is the highest amongst the Period 2 homonuclear diatomic molecules. N_2 shows a highly negative Laplacian value at the bond critical point, indicating its covalent nature. Ne_2 is most weakly bound amongst the Period 2 diatomic molecules. Figure 7 shows the differences in the 2D contour plot of electron density between N_2 and Ne_2. The contour shows the clear differences between the covalent and van der Waals bonds. In case of Ne_2 the signature of the individual's atoms electron density is preserved, with negligible amount of overlap between the atoms contours.

3.10 *Comparison between N_2, O_2 and F_2 based on the Laplacian of electron density contour map*

N_2, O_2 and F_2 are typically described as having a triple, double and single bonded diatomic molecules. Binding energy, as well as electron density at bond critical point, decreases from N_2 to F_2. Laplacian of electron density is negative for N_2 (−3.5009) and O_2 (−0.9375). However for F_2, the Laplacian of the electron density ($\nabla^2\rho$) at the

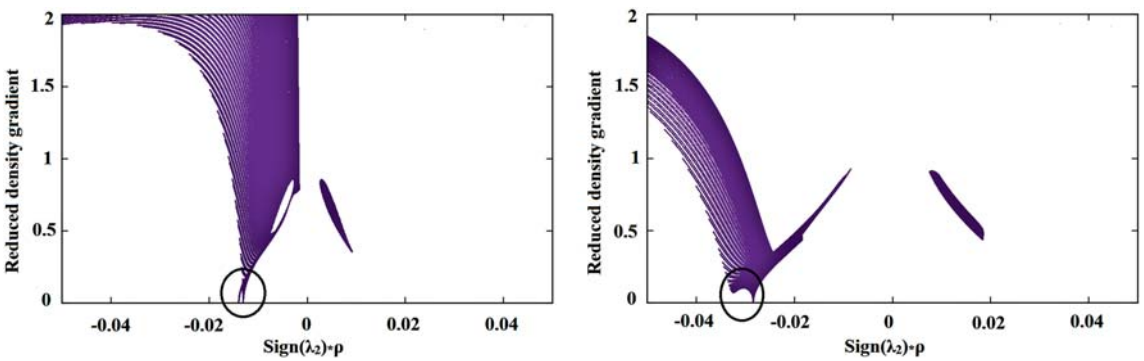

Figure 6. Non-covalent index plots for Li_2 (left) and Be_2 (right). X-axis is the reduced density gradient and Y-axis is $\text{sign}(\lambda_2)*\rho$.

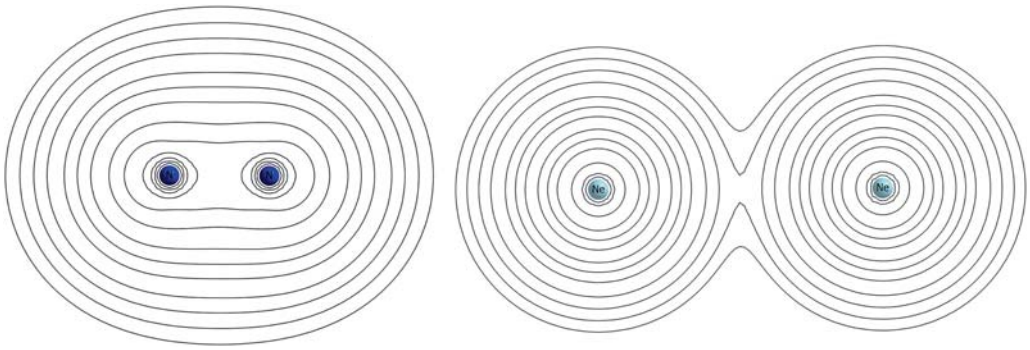

Figure 7. 2D contour of ρ(r) for N_2, a typical example of a covalent bond (above) and Ne_2, a typical example of van der Waals (below) molecule.

BCP is positive unlike what is expected for shared-shell interaction, a normal covalent bond. Positive $\nabla^2\rho$ essentially means electron depletion around the BCP. In a general term, the formation of a covalent bond accumulates electron density around the bond critical points (as can be seen in case of N_2 and O_2), but in F_2 where the atoms are very electronegative, electron density is strongly pulled toward the nuclei which essentially weakens the F–F bond. Figure 8 shows the $\nabla^2\rho$ contour plots for N_2, O_2, F_2, the contours for N_2 and O_2 are similar, having large negative values around the internuclear region. Whereas, in F_2, the negative $\nabla^2\rho$ region is only around the F atoms, in the internuclear region there is a large positive $\nabla^2\rho$ space. This kind of anomaly is also present in H_2O_2. $\nabla^2\rho$ at the O-O bcp is indeed positive in H_2O_2.[96] So, sign of $\nabla^2\rho$ is not a definitive criterion to differentiate between ionic and covalent interactions. For F_2, both $|\lambda_1|/\lambda_3$ and $|V|/G$ ratios are intermediate range of closed and shared interactions.

3.11 *Potential acting on one electron in a molecule*

Zhao and Yang[76] showed that the potential acting on one electron in a molecule (PAEM) can give us a clear distinction between the chemical bond and van der Waals interactions. As we propose all the diatomic molecules are bound by 'chemical bonds', we prefer to use the terminology 'shared' and 'closed' for PAEM analysis. The PAEM is defined as the interaction energy of one electron at local position $\overrightarrow{r}$ with the remaining electrons and all the nuclei in a molecular system:

$$V_{PAEM}(\overrightarrow{r}) = -\sum_A \frac{Z_A}{\left|\overrightarrow{r} - \overrightarrow{R_A}\right|} + \frac{1}{\rho(\overrightarrow{r})}\int \frac{\rho_2(\overrightarrow{r},\overrightarrow{r_2})}{\left|\overrightarrow{r} - \overrightarrow{r_2}\right|} d\overrightarrow{r_2}$$

where Z_A and $\overrightarrow{R_A}$ are the nuclear charge and position of nucleus A, $\rho(\overrightarrow{r})$ the electron density, $\rho_2(\overrightarrow{r},\overrightarrow{r_2})$ is the two-electron density function, that is, the probability function of finding one electron at $\overrightarrow{r}$ and another electron at $\overrightarrow{r_2}$ simultaneously. $\rho(\overrightarrow{r})$and $\rho_2(\overrightarrow{r},\overrightarrow{r_2})$ are accurately expressed by the electronic wave function. In this work, we have evaluated the wave function at CCSD (t,full)/aug-cc-pVTZ level.

Based on PAEM, $V(\overrightarrow{r})$, we can define the force acting on one electron in a molecule (FAEM), which is just the minus of the gradient of the PAEM, that is

$$F(\overrightarrow{r}) = -\nabla V(\overrightarrow{r})$$

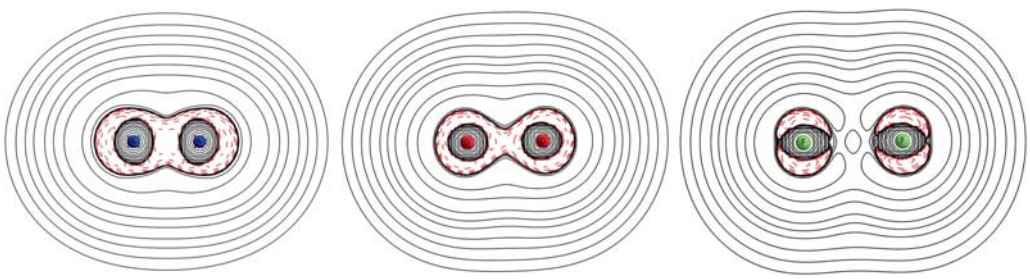

Figure 8. Contour plots of $\nabla^2\rho$ of N_2, O_2 and F_2. Red color denotes the negative region and the black represents the positive region. The internuclear region $\nabla^2\rho$ has a large negative value for N_2 and O_2 (red curves).Whereas for F_2, $\nabla^2\rho$ in the internuclear region is positive (black curve).

Table 15. Molecular orbitals and energy levels for Be_2 and Ne_2. (Bold values are for filled orbital). Energies are in a.u.

Diatomic molecules	σ_{1s}	σ_{1s*}	σ_{2s}	σ_{2s*}	σ_{2p}	π_{2p}	σ_{2p*}	π_{2p*}
Be_2	**−4.731**	**−4.731**	**−0.405**	**−0.238**	0.005	0.008	0.024	0.036
	σ_{1s}	σ_{1s*}	σ_{2s}	σ_{2s*}	σ_{2p}	π_{2p}	π_{2p*}	σ_{2p*}
Ne_2	**−32.779**	**−32.779**	**−1.934**	**−1.933**	**−0.855**	**−0.852**	**−0.850**	**−0.847**

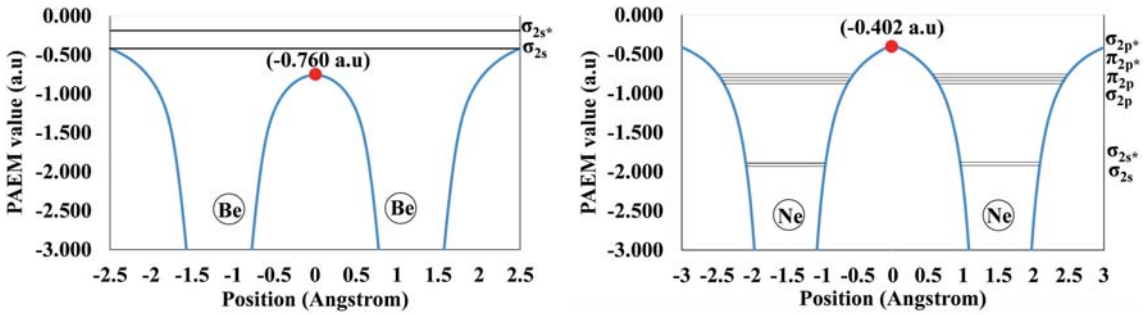

Figure 9. The PAEM-MO diagram along the line connecting two atoms: (a) Be_2 molecule, shared shell (chemical bonding) interaction; (b) Ne_2 molecule closed-shell (van der Waals) interaction.

Table 16. Potential acting on one electron (PAEM), electrostatic potential (ESP) and electron density at BCP for Period 2 homonuclear diatomic molecules (values are in a.u).

Diatomic molecules	PAEM (a.u)	Energy of the HOMO (a.u)	Nature of interaction	ESP (a.u)	Electron density at BCP (a.u)
Li_2	−0.452	−0.182	Shared	0.103	0.0130
Be_2	−0.760	−0.238	Shared	0.256	0.0373
B_2	−1.564	−0.363	Shared	0.811	0.1247
C_2	−2.484	−0.457	Shared	1.518	0.3160
N_2	−3.240	−0.614	Shared	1.843	0.7204
O_2	−2.777	−0.560	Shared	1.448	0.5505
F_2	−1.940	−0.667	Shared	0.809	0.3004
Ne_2	−0.402	−0.847	Closed	0.033	0.0023

Values of $V(\overrightarrow{r})$and $F(\overrightarrow{r})$at each point of $\overrightarrow{r}$ can be worked out with numerical calculations in terms of an *ab initio* method. A point where $F(\overrightarrow{r})$ is equal to zero is called a critical point of the PAEM.

Multiwfn 3.6[84] was used to calculate PAEM. The MO's are calculated at CCSD(t)(full)/aug-cc-pVTZ level given in Table 15. For Be_2, σ2 s and σ2 s* MO's are above the PAEM barrier (−0.76 a.u ∼ −21 ev), see Figure 9. So the electrons can freely interflow between the two Be atoms. Whereas in Ne_2 all the MOs are below the PAEM barrier (−0.40 a.u ∼ −11 ev). This means that the PAEM barrier in Ne_2, separates Ne_2 into two Ne atoms between which the electron interflow does not exist except by tunnelling. A similar analysis has been carried out for other diatomic molecules and the results are provided in Table 16.

3.12 *Total electrostatic potential*

The electrostatic potential, ESP, measures the potential energy that a positive test unit charge (not belonging to the molecular system) gains on being transported from infinity to point r:

$$V_{esp}(\overrightarrow{r}) = \sum_A \frac{Z_A}{\left|\overrightarrow{r} - \overrightarrow{R_A}\right|} - \int \frac{\rho(\overrightarrow{r_2})}{\left|\overrightarrow{r} - \overrightarrow{r_2}\right|} d\overrightarrow{r_2}$$

A runs over all the nuclei of the molecule and Z_A is the nuclear charge of a nucleus at R_A.

$$V_{PAEM}(\overrightarrow{r}) = -V_{ESP}(\overrightarrow{r}) + \frac{V_{xc}(\overrightarrow{r})}{\rho(\overrightarrow{r})}$$

V_{xc} is the two-electron contribution from the quantum exchange-correlation potential.

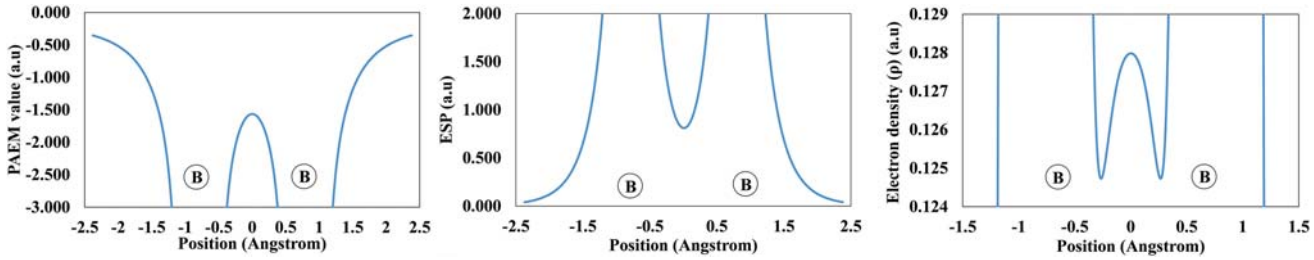

Figure 10. A typical example of PAEM (left), ESP (middle) and electron density (right) at BCP for B_2 molecule.

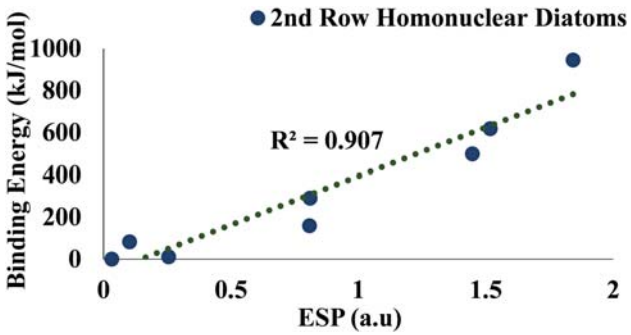

Figure 11. Correlation plot of Binding Energy vs. ESP for Period 2 homonuclear dimer.

$$V_{xc} = \frac{1}{\rho(\overrightarrow{r})} \int \frac{\rho_{xc}(r, r_2)}{|\overrightarrow{r} - \overrightarrow{r_2}|} dr_2$$

From Figure 10, it can be realised that PAEM and ESP are of opposite signs. Electron density shows two minima along the bond for B_2 at CCSD(T) level but the PAEM and ESP shows only one maxima and minima along the internuclear region. In Table 16 PAEM, ESP and electron density values are reported for the Period 2 diatomic molecules. PAEM and ESP are well correlated with each other which indicates quantum exchange-correlation potential scales linearly with the values (Figure SF7, Supplementary Information). For both HLi and HF, the PAEM barrier is lower compared to the major valence bonding orbital in both the cases (Figure SF6, Supplementary Information). Natural resonance theory (NRT)[83] is used to measure the covalency and ionicity in these bonds. NRT shows LiH is 85% ionic and HF is 57% ionic (Table ST13, Supplementary Information).

For Li_2 to F_2, except σ_{1s} and σ_{1s^*}, all other molecular orbitals are above the PAEM barrier. However, for Ne_2 all the energy levels are below the PAEM barrier. In fact, the binding energy correlates well with ESP having R^2 of around 0.91 (Figure 11). There is a good correlation between the PAEM and ESP at their critical points between the two atoms and hence between the binding energy and ESP as well. These are shown in Figures SF7 and SF8 in Supplementary Information. Clearly, the PAEM analysis allows us to compare the bonding in all 8 homonuclear diatomic molecules from Period 2 as one group, unlike the electron density at the BCP based on AIM analysis, in which these had to be grouped into three sets.

4. Conclusions

Chemical bonding is indeed a highly complex phenomenon. Period 2 homonuclear diatomic molecules exhibit all the diversity in chemical bonds that can be observed. We can summarize the results of our analysis in the following points:

1. AIM analysis reveals that Li_2, B_2 and C_2 have a non-nuclear critical point at the midpoint. For B_2 and C_2 the appearance of the non-nuclear critical point is sensitive towards the nature of wave functions. The topological properties at the bond critical point for these molecules may not be good indicators of the nature of the interaction.
2. For N_2, O_2, F_2, a typical bond critical point in the internuclear region is found. However, for F_2, $\nabla^2\rho$ at bond critical point is positive, suggesting electron depletion around the bond critical point. However, the PAEM-MO suggests that F_2 has a shared-shell (covalent) bond as expected whereas Ne_2 has a closed-shell bond. Non-Covalent Index plot also shows closed-shell bonding in Ne_2 molecule (Figure SF4, Supplementary Information).
3. To understand two different regimes of bonding namely ionic and covalent bonds, we have analyzed the bonding properties of LiH and HF. $\nabla^2\rho$ plot clearly reflects the differences between the two. For LiH, $\nabla^2\rho$ is positive at BCP, indicating ionic bond whereas, $\nabla^2\rho$ negative at BCP for HF, indicating covalent bond. However, NRT analysis revels HLi is 85% ionic and HF is 57% ionic.
4. Finally, the AIM analysis shows that Period 2 diatomic molecules can be grouped into three different types based on the correlation between

binding energy and electron density at the BCP. One group (Li_2, B_2 and C_2) shows NNA in between the two atoms. Both PAEM and ESP analysis indicate only one critical point between the two atoms for all the eight Period 2 diatomic molecules and the values calculated at these critical points have strong correlation with the binding energy covering three orders of magnitude. While this could be used by some to argue that, electrostatics can explain all bonding, one should not forget that these values have been calculated by accurate quantum mechanical methods that take into account electrostatics, dispersion, charge transfer-covalency and exchange repulsion.

Supplementary Information (SI)

Thirteen tables and nine figures have been provided in the Supplementary Information. Method and basis set dependence of Be_2 distance (Table ST1), electron density topological properties of all the Group II homonuclear diatomic molecules (Tables ST2–ST9), electron density on atoms and NNA for Li_2, B_2 and C_2 at CCCD/aug-cc-pVTZ level (Table ST10), changes in atomic properties calculated by AIM (Table ST11), ground and low lying excited states of B_2 and C_2 (Table ST12) and iconicity and covalency of LiH and HF by NRT analysis (Table ST13). Bar diagram showing percentage errors in diatom dissociation energy at various level (Figure SF1), correlation between binding energy and electron density at the BCP for Period 2 homonuclear diatomic molecules (Figure SF2), $|\lambda 1|/\lambda 3$ and $|V|/G$ ratio for homonuclear diatomic molecules (Figure SF3), NCI plot for Ne_2 (Figure SF4), variation of the electron density (ρ) along the internuclear axis of LiH and HF (Figure SF5), PAEM-MO diagram along the line connecting two atoms: for LiH and HF (Figure SF6), correlation plot between |PAEM| and ESP for homonuclear diatomic molecules of Period 2 (Figure SF7) and correlation plot between binding energy vs. |PAEM| for homonuclear diatomics of Period 2 (Figure SF8). Full Reference of 79 provided in supporting information.

Acknowledgements

Computational facilities at the Department of Inorganic and Physical Chemistry maintained by Prof. Sai G. Ramesh is acknowledged. AD acknowledges the Indian Institute of Science for the research fellowship.

References

1. Herzberg G and Mrozowski S 1951 Molecular spectra and molecular structure. I. Spectra of diatomic molecules *Am. J. Phys.* **19** 390
2. Huber K P and Herzberg G 1979 *Molecular Structure and Molecular Spectra. IV. Constants of Diatomic Molecules* (New York: Van Rostrand-Reinhold)
3. Arunan E, Desiraju G R, Klein R A, Sadlej J, Scheiner S, Alkorta I, Clary D C, Crabtree R H, Dannenberg J J, Hobza P, Kjaergaard H G, Legon A C, Mennucci B and Nesbitt D J 2011 Definition of the hydrogen bond (IUPAC Recommendations 2011) *Pure Appl. Chem.* **83** 1637
4. Arunan E, Desiraju G R, Klein R A, Sadlej J, Scheiner S, Alkorta I, Clary D C, Crabtree R H, Dannenberg J J, Hobza P, Kjaergaard H G, Legon A C, Mennucci B and Nesbitt D J 2011 Defining the hydrogen bond: An account (IUPAC Technical Report) *Pure Appl. Chem.* **83** 1619
5. Legon A C 2010 The halogen bond: An interim perspective *Phys. Chem. Chem. Phys.* **12** 7736
6. Metrangolo P and Resnati G 2001 Halogen Bonding: A Paradigm in Supramolecular Chemistry *Chem. – A Eur. J.* **7** 2511
7. Alkorta I, Blanco F, Solimannejad M and Elguero J 2008 Competition of hydrogen bonds and halogen bonds in complexes of hypohalous acids with nitrogenated bases *J. Phys. Chem. A* **112** 10856
8. Clark T, Hennemann M, Murray J S and Politzer P 2007 Halogen bonding: The σ-hole *J. Mol. Model.* **13** 291
9. Wang W, Ji B and Zhang Y 2009 Chalcogen bond: A sister noncovalent bond to halogen bond *J. Phys. Chem. A* **113** 8132
10. Manna D and Mugesh G 2012 Regioselective deiodination of thyroxine by iodothyronine deiodinase mimics: An unusual mechanistic pathway involving cooperative chalcogen and halogen bonding *J. Am. Chem. Soc.* **134** 4269
11. Bleiholder C, Werz D B, Köppel H and Gleiter R 2006 Theoretical investigations on chalcogen − chalcogen interactions: What makes these nonbonded interactions bonding? *J. Am. Chem. Soc.* **128** 2666
12. Sanz P, Mó O and Yáñez M 2003 Characterization of intramolecular hydrogen bonds and competitive chalcogen–chalcogen interactions on the basis of the topology of the charge density *Phys. Chem. Chem. Phys.* **5** 2942
13. Del Bene J E, Alkorta I, Sanchez-Sanz G and Elguero J 2011 Structures, energies, bonding, and NMR properties of pnicogen complexes $H_2XP{:}NXH_2$ (X = H, CH_3, NH_2, OH, F, Cl) *J. Phys. Chem. A* **115** 13724
14. Zahn S, Frank R, Hey-Hawkins E and Kirchner B 2011 Pnicogen bonds: A new molecular linker? *Chem. Eur. J.* **17** 6034
15. Scheiner S 2011 A new noncovalent force: Comparison of P···N interaction with hydrogen and halogen bonds *J. Chem. Phys.* **134** 94315
16. Mani D and Arunan E 2013 The X–C···Y (X = O/F, Y = O/S/F/Cl/Br/N/P) 'carbon bond' and hydrophobic interactions *Phys. Chem. Chem. Phys.* **15** 14377
17. Mani D and Arunan E 2014 The X–C··· π (X = F, Cl, Br, Cn) carbon bond *J. Phys. Chem. A* **118** 10081
18. Thomas S P, Pavan M S and Guru Row T N 2014 Experimental evidence for 'carbon bonding' in the solid state from charge density analysis *Chem. Commun.* **50** 49

19. Bauzá A, Mooibroek T J and Frontera A 2013 Tetrel-bonding interaction: Rediscovered supramolecular force? *Angew. Chemie - Int. Ed.* **52** 12317
20. Grabowski S J 2014 Tetrel bond–σ-hole bond as a preliminary stage of the S_N2 reaction *Phys. Chem. Chem. Phys.* **16** 1824
21. Grabowski S J 2014 Boron and other triel Lewis acid centers: From hypovalency to hypervalency *ChemPhysChem* **15** 2985
22. Kollman P A, Liebman J F and Allen L C 1970 Lithium bond *J. Am. Chem. Soc.* **92** 1142
23. Ault B S and Pimenter G C 1975 Matrix isolation infrared studies of lithium bonding *J. Phys. Chem.* **79** 621
24. McCleskey T M, Ehler D S, Keizer T S, Asthagiri D N, Pratt L R, Michalczyk R and Scott B L 2007 Beryllium displacement of H + from strong hydrogen bonds *Angew. Chemie* **119** 2723
25. Albrecht L, Boyd R J, Mó O and Yáñez M 2012 Cooperativity between hydrogen bonds and beryllium bonds in (H2O)nBeX2 (n = 1–3, X = H, F) complexes. A new perspective *Phys. Chem. Chem. Phys.* **14** 14540
26. Dunlap B I, Connolly J W D and Sabin J R 1979 On first-row diatomic molecules and local density models *J. Chem. Phys.* **71** 4993
27. Hajigeorgiou P G 2010 An extended Lennard-Jones potential energy function for diatomic molecules: Application to ground electronic states *J. Mol. Spectrosc.* **263** 101
28. Peterson K A, Kendall R A and Dunning T H 1993 Benchmark calculations with correlated molecular wave functions. III. Configuration interaction calculations on first row homonuclear diatomics *J. Chem. Phys.* **99** 9790
29. Peterson K A, Wilson A K, Woon D E and Dunning Jr. T H 1997 Benchmark calculations with correlated molecular wave functions XII. Core correlation effects on the homonuclear diatomic molecules B2-F2 *Theor. Chem. Acc.* **97** 251
30. Binkley J S and Frisch M J 1983 ab initio determination of bond dissociation energies: The first-row diatomics co, N2, NO, O2, and F2 *Int. J. Quantum Chem.* **24** 331
31. Painter G S and Averill F W 1982 Bonding in the first-row diatomic molecules within the local spin-density approximation *Phys. Rev. B* **26** 1781
32. Ghanty T K and Ghosh S K 1991 Electronegativity and covalent binding in homonuclear diatomic molecules *J. Phys. Chem.* **95** 6512
33. Müller T, Dallos M, Lischka H, Dubrovay Z and Szalay P G 2001 A systematic theoretical investigation of the valence excited states of the diatomic molecules B_2, C_2, N_2 and O_2 *Theor. Chem. Acc.* **105** 227
34. Wang J, Clark B J, Schmider H and Smith V H 1996 Topological analysis of electron momentum densities and the bond directional principle: The first-row hydrides, AH, and homonuclear diatomic molecules, A2 *Can. J. Chem.* **74** 1187
35. Driessler F and Kutzelnigg W 1976 Analysis of the chemical bond *Theor. Chim. Acta* **43** 1
36. Bradley C C, Sackett C A, Tollett J J and Hulet R G 1995 Evidence of Bose-Einstein condensation in an atomic gas with attractive interactions *Phys. Rev. Lett.* **75** 1687
37. Bradley C C, Sackett C A and Hulet R G 1997 Bose-Einstein condensation of lithium: Observation of limited condensate number *Phys. Rev. Lett.* **78** 985
38. Herzberg G 1929 Zum Aufbau der zweiatomigen Moleküle *Zeitschrift für Phys.* **57** 601
39. Herzberg L 1933 Über ein neues Bandensystem des Berylliumoxyds und die Struktur des Be O-Moleküls *Zeitschrift für Phys.* **84** 571
40. Bondybey V E and English J H 1984 Laser vaporization of beryllium: Gas phase spectrum and molecular potential of Be2 *J. Chem. Phys.* **80** 568
41. Merritt J M, Bondybey V E and Heaven M C 2009 Beryllium Dimer—Caught in the act of bonding *Science* **324** 1548
42. Douglas A E and Herzberg G 1940 Spectroscopic evidence of the B2 molecule and determination of its structure *Can. J. Res.* **18** 165
43. Graham W R M and Weltner W 1976 B atoms, B2 and H2BO molecules: ESR and optical spectra at 4 °K *J. Chem. Phys.* **65** 1516
44. Dupuis M and Liu B 1978 The ground electronic state of B_2 *J. Chem. Phys.* **68** 2902
45. Langhoff S R and Bauschlicher Jr C W 1991 Theoretical study of the spectroscopy of B_2 *J. Chem. Phys.* **95** 5882
46. Boggio-Pasqua M, Halvick P, Rayez M-T, Rayez J-C and Robbe J-M 1998 Ab initio study of the potential energy surfaces for the reaction $C + CH \rightarrow C_2 + H$ *J. Phys. Chem. A* **102** 2009
47. Martin M 1992 C2 spectroscopy and kinetics *J. Photochem. Photobiol. A Chem.* **66** 263
48. Van Orden A and Saykally R J 1998 Small carbon clusters: Spectroscopy, structure, and energetics *Chem. Rev.* **98** 2313
49. Boggio-Pasqua M, Voronin A I, Halvick P and Rayez J-C 2000 Analytical representations of high level ab initio potential energy curves of the C2 molecule *J. Mol. Struct. THEOCHEM* **531** 159
50. Weltner Jr W and Van Zee R J 1989 Carbon molecules, ions, and clusters *Chem. Rev.* **89** 1713
51. Douay M, Nietmann R and Bernath P F 1988 The discovery of two new infrared electronic transitions of C2: B1Δg-A1Πu and B′ 1Σg + -A1Πu *J. Mol. Spectrosc.* **131** 261
52. Douay M, Nietmann R and Bernath P F 1988 New observations of the A1Πu-X1Σg + transition (Phillips system) of C2 *J. Mol. Spectrosc.* **131** 250
53. Pradhan A D, Partridge H and Bauschlicher C W 1994 The dissociation energy of CN and C2 *J. Chem. Phys.* **101** 3857
54. Mulliken R S 1939 Note on electronic states of diatomic carbon, and the carbon-carbon bond *Phys. Rev.* **56** 778
55. Su P, Wu J, Gu J, Wu W, Shaik S and Hiberty P C 2011 Bonding conundrums in the C2 molecule: A valence bond study *J. Chem. Theory Comput.* **7** 121
56. Shaik S, Danovich D, Wu W, Su P, Rzepa H S and Hiberty P C 2012 Quadruple bonding in C 2 and analogous eight-valence electron species *Nat. Chem.* **4** 195

57. von RaguéSchleyer P, Maslak P, Chandrasekhar J and Grev R S 1993 Is a CC quadruple bond possible? *Tetrahedron Lett.* **34** 6387
58. Lofthus A and Krupenie P H 1977 The spectrum of molecular nitrogen *J. Phys. Chem. Ref. Data* **6** 113
59. Huber K-P 2013 *Molecular Spectra and Molecular Structure: IV. Constants of Diatomic Molecules* (Location: Springer Science & Business Media)
60. Krupenie P H 1972 The spectrum of molecular oxygen *J. Phys. Chem. Ref. Data* **1** 423
61. Matsunaga F M and Watanabe K 1967 Total and photoionization coefficients and dissociation continua of O_2 in the 580–1070 Å region *Sci. Light* **16** 31
62. Gale H G and Monk G S 1924 The spectrum of fluorine *Astrophys. J.* **59** 125
63. Gale H G and Monk G S 1929 The band spectrum of fluorine *Astrophys. J.* **69** 77
64. Andrychuk D 1951 The Raman spectrum of fluorine *Can. J. Phys.* **29** 151
65. Tanaka Y and Yoshino K 1972 Absorption spectra of Ne2 and HeNe molecules in the vacuum-uv region *J. Chem. Phys.* **57** 2964
66. Pauling L 1960 *The Nature of the Chemical Bond* (Ithaca, NY: Cornell University Press)
67. Bader R F W, Keaveny I and Cade P E 1967 Molecular charge distributions and chemical binding. II. First-row diatomic hydrides, AH *J. Chem. Phys.* **47** 3381
68. Bader R F W 1990 *Atoms in Molecules: A Quantum Theor*y (New York: Oxford University Press)
69. Popelier P L A, Aicken F M and O'Brien S E 2000 Atoms in molecules *Chem. Model. Appl. Theory* **1** 143
70. Amezaga N J M, Pamies S C, Peruchena N M and Sosa G L 2009 Halogen bonding: A study based on the electronic charge density *J. Phys. Chem. A* **114** 552
71. Cremer D and Kraka E 1984 Chemical bonds without bonding electron density—Does the difference electron-density analysis suffice for a description of the chemical bond? *Angew. Chem. Int. Ed. Eng.* **23** 627
72. Johnson E R, Keinan S, Mori-Sanchez P, Contreras-Garcia J, Cohen A J and Yang W 2010 Revealing noncovalent interactions *J. Am. Chem. Soc.* **132** 6498
73. Contreras-García J, Yang W and Johnson E R 2011 Analysis of hydrogen-bond interaction potentials from the electron density: Integration of noncovalent interaction regions *J. Phys. Chem. A* **115** 12983
74. Contreras-García J, Johnson E R, Keinan S, Chaudret R, Piquemal J-P, Beratan D N and Yang W 2011 NCIPLOT: A program for plotting noncovalent interaction regions *J. Chem. Theory Comput.* **7** 625
75. Zhao D-X and Yang Z-Z 2014 Theoretical exploration of the potential and force acting on one electron within a molecule *J. Phys. Chem. A* **118** 9045
76. Zhao D and Yang Z 2014 Investigation of the distinction between van der Waals interaction and chemical bonding based on the PAEM-MO diagram *J. Comput. Chem.* **35** 965
77. Zhao D, Gong L and Yang Z 2002 Exploration of the potential acting on an electron within diatomic molecules *Chin. Sci. Bull.* **47** 635
78. Bartashevich E and Tsirelson V 2018 A comparative view on the potential acting on an electron in a molecule and the electrostatic potential through the typical halogen bonds *J. Comput. Chem.* **39** 573
79. Frisch M J, Trucks G W, Schlegel H B, Scuseria G E, Robb M A, Cheeseman J R, Scalmani G, Barone V, Mennucci B and Petersson G A 2009 *Gaussian 09 Revision D. 01, 2009* (Wallingford CT: Gaussian Inc.)
80. Werner H J, Knowles P J, Knizia G, Manby F R, Schütz M, Celani P, Györffy W, Kats D, Korona T and Lindh R 2015 *MOLPRO, Version 2015.1, a Package of Ab Initio Programs* (Cardiff, Wales, UK: Univ. Cardiff Chem. Consult.)
81. Keith T A 2014 AIMAll (Version 14.11.23), TK Gristmill Software, Overland Park KS, USA
82. Glendening E D, Landis C R and Weinhold F 2013 NBO 6.0: Natural bond orbital analysis program *J. Comput. Chem.* **34** 1429
83. Glendening E D and Weinhold F 1998 Natural resonance theory: I. General formalism *J. Comput. Chem.* **19** 593
84. Lu T and Chen F 2012 Multiwfn: A multifunctional wavefunction analyzer *J. Comput. Chem.* **33** 580
85. Bacskay G B and Nordholm S 2017 Covalent bonding in the hydrogen molecule *J. Phys. Chem. A* **121** 9330
86. Aziz R A and Slaman M J 1989 The Ne-Ne interatomic potential revisited *Chem. Phys.* **130** 187
87. Emsley J 1998 *The Elements* (Oxford; New York: Clarendon Press; Oxford University Press)
88. Heaven M C, Bondybey V E, Merritt J M and Kaledin A L 2011 The unique bonding characteristics of beryllium and the Group IIA metals *Chem. Phys. Lett.* **506** 1
89. Luo Y-R 2003 *Handbook of Bond dissociation energies In Organic Compounds* (Boca Raton: CRC Press) p. 89
90. Sudhakar P V and Lammertsma K 1993 Bond properties of Be3–7 clusters *J. Chem. Phys.* **99** 7929
91. Cao W L, Gatti C, MacDougall P J and Bader R F W 1987 On the presence of non-nuclear attractors in the charge distributions of Li and Na clusters *Chem. Phys. Lett.* **141** 380
92. Vries R Y de, Briels W J, Fell D, Velde G te and Baerends E J 1996 Charge density study with the Maximum Entropy Method on model data of silicon. A search for non-nuclear attractors *Can. J. Chem.* **74** 1054
93. Iversen B B, Larsen F K, Souhassou M and Takata M 1995 Experimental evidence for the existence of non-nuclear maxima in the electron-density distribution of metallic beryllium. A comparative study of the maximum entropy method and the multipole refinement method *Acta Crystallogr. Sect. B* **51** 580
94. Platts J A, Overgaard J, Jones C, Iversen B B and Stasch A 2010 First experimental characterization of a non-nuclear attractor in a dimeric magnesium (I) compound *J. Phys. Chem. A* **115** 194
95. Brea O and Corral I 2018 Super strong Be–Be bonds: Theoretical insight into the electronic structure of Be–Be complexes with radical ligands *J. Phys. Chem. A* **122** 2258
96. Mó O, Yáñez M, Eckert-Maksić M, Maksić Z B, Alkorta I and Elguero J 2005 Periodic trends in bond dissociation energies. A theoretical study *J. Phys. Chem. A* **109** 4359